Microfluid Nanofluid
DOI 10.1007/s10404-013-1247-0

RESEARCH PAPER

Brownian motion-induced water slip inside carbon nanotubes

Chao Chen · Luming Shen · Ming Ma · Jefferson Zhe Liu · Quanshui Zheng

Received: 25 September 2012 / Accepted: 9 August 2013

Abstract Molecular dynamics simulations are performed to understand the characteristics of the one-dimensional Brownian motion of water columns inside carbon nanotubes (CNTs) at room temperature. It is found that the probability of 2–10-nm-long water columns sliding a distance larger than the energy barrier period inside 2–5-nm-diameter CNTs is greater than 50 %. Moreover, a conservative estimation gives that the thermal fluctuation-induced driving force exceeds the upper bound of the sliding energy barrier for a water column shorter than 117 nm. These findings imply that although water molecules form layered structures near the CNT inner walls, there is no critical interfacial shear stress to conquer, and water could slip inside CNTs under any given pressure drop due to the thermal activation at room temperature.

C. Chen · Q. Zheng
Department of Engineering Mechanics, Tsinghua University, Beijing 100084, China

C. Chen · L. Shen (✉)
School of Civil Engineering, University of Sydney, Sydney, NSW 2006, Australia
e-mail: Luming.Shen@sydney.edu.au

C. Chen · Q. Zheng (✉)
Center for Nano and Micro Mechanics, Tsinghua University, Beijing 100084, China
e-mail: zhengqs@tsinghua.edu.cn

M. Ma
Department of Chemistry, London Centre for Nanotechnology, University College London, London WC1H 0AJ, UK

J. Z. Liu
Department of Mechanical and Aerospace Engineering, Monash University, Clayton, VIC 3800, Australia

Keywords One-dimensional Brownian motion · Nanoscale flow · Liquid slip · Carbon nanotubes · Molecular dynamics

1 Introduction

Understanding nanoscale interaction between liquid and solid interfaces is crucial to many novel applications, such as micro- and nanofluidic design (Stone et al. 2004) and self-cleaning effect devices (Barthlott and Neinhuis 1997). Recently, scientists have found that the measured water flow flux through nanochannels of carbon nanotubes (CNTs) membranes could be 3–5 orders larger than the theoretical prediction with nonslip assumption (Majumder et al. 2005; Holt et al. 2006). The surprising enhancement was attributed to the large flow slip occurring at the liquid–solid interface, which makes high-speed liquid transportation possible through nanoscale channels (Chen et al. 2011). Slip phenomena can also be observed in bio-environment, where a recent experiment has confirmed that large slip can occur when water flows through nanoscale protein channels (Peng et al. 2009).

Many molecular dynamics (MD) simulations of water flow through CNTs have been carried out to quantitatively study the slip properties at nanoscale in the past few years. Thompson and Troian (1997) proposed a nonlinear slip length and shear rate relationship: $l_s = l_{s0}(1 - \gamma/\gamma_c)^{-\alpha}$, where l_s is the slip length, γ the shear rate, l_{s0} the asymptotic limiting value of l_s, γ_c the critical shear rate, and α the constant depending on the properties of liquid and solid, which was significantly different from the classical Navier linear slip assumption. Chen et al. (2008) suggested a parabolic relationship between slip velocity and shear stress based on the MD simulation data for flow velocity

Published online: 24 August 2013

ranging from ~5 to ~275 m/s. Through MD simulations of a relatively large water flow range (0.33–1,400 m/s), Ma et al. (2011) confirmed that there exists an inverse hyperbolic sine function between the friction stress and flow velocity in double-walled CNTs, which is consistent with the transition state theory (Yang 2009). Xiong et al. (2011) further found that the inverse hyperbolic function applied in graphene nanochannels as well.

All the above-mentioned studies suggest that the shear stress τ versus slip velocity v curve should pass through the origin point (0, 0) in the $\tau \sim v$ plot, which implies the liquid would slip under any given pressure drop. However, there is no consensus on the underlying physics of the nanoscale flow slipping at solid surfaces. It has been demonstrated that liquid molecules can form layered structure next to solid surface due to the intermolecular interactions between the liquid and the solid (Mo et al. 2005). The thickness of the layered structure is usually larger than 0.5 nm. It is thus intuitive from the perspective of molecular level to assume that the friction force between the layered liquid and the solid surface would behave like the solid–solid interaction. Therefore, there could be a critical shear force at the liquid–solid surface interfaces, just like at the solid–solid interfaces, before nanoscale flow slip could occur at the solid surface. Martini et al. (2008) found that there is a transition from nonslip to slip flow in a Lennard–Jones fluid when the shear rates increase from zero. The transition occurs at a relatively high flow speed (~30 m/s) due to the strong fluid–wall interaction used, which is significantly different from water flowing inside CNTs where the water–carbon interaction is much weaker. Limited by the computational capability and thermal fluctuation, it is difficult in the MD simulations to decrease the flow speed unlimitedly down to zero to explicitly investigate the ultra-slow water flows. An intuitive picture of the randomly moving water molecules above the carbon wall was depicted in Ma et al. (2011) to support the assumption of the negligible critical shear stress. In the current study, we carry out MD simulations of the one-dimensional spontaneous thermal motion of water columns inside CNTs in order to compare the magnitudes of the thermal fluctuation-induced driving force for water flow and the resistance force due to water–CNT interactions and to understand the molecular mechanism of water slip at the atomically smooth graphene surfaces under room temperature.

One-dimensional Brownian motion has been widely studied for several decades. Based on the classical Langevin theory (Pathria 1996), a single particle exhibits diffusion property $\langle \Delta x^2 \rangle \propto t$, namely the averaged mean square displacement $\langle \Delta x^2 \rangle$ linearly increases with time t, when the observation period exceeds a critical value. For a time scale smaller than the critical value, the single particle will move at a constant speed. Meanwhile, the short-term behavior of single-file water molecules is rarely concerned because of the relatively less significance, and the difficulties in the experimental observation for the extremely short period (~picoseconds). However, it carries the crucial thermal fluctuation information that may serve as the key point for understanding the water slip phenomena at nanoscale.

The current work investigates the fundamental one-dimensional Brownian motion behavior of water columns slip inside CNTs. We will establish the dependence of the one-dimensional Brownian motion of water columns on the parameters such as nanotube size, temperature T and contact angle θ_{CA} and determine the effect of water column length on the thermal fluctuation-induced driving force and the water–CNT interaction-based resistance force for water motion. Furthermore, the lower bound of the critical water column length, under which the slip of water will spontaneously occur inside CNT surface at room temperature, is estimated. This new finding confirms that the critical shear stress for water slip over atomically smooth surfaces is absent because of the thermal fluctuation-induced driving force at room temperature.

2 Simulation procedure

We used the MD simulation package large-scale atomic/molecular massively parallel simulator (LAMMPS) (Plimpton 1995) to study the slip behavior of water columns inside CNTs (Fig. 1). In our MD simulations, single-walled armchair CNTs were adopted to serve as flow channels with atomically smooth surface. The periodic boundary condition was enforced in the axial direction of the CNTs. The adaptive intermolecular reactive empirical bond order (AIREBO) force field (Stuart et al. 2000) was applied to describe the interaction of carbon atoms of the CNTs. An extended simple point charge (SPC/E) model (Berendsen et al. 1987) was used to describe the interactions between the water molecules. The viscosity of water calculated from the SPC/E model at room temperature 298 K is 0.729 mPa s (Gonzalez and Abascal 2010) and surface tension 63.6 mJ/m^2 (Markesteijn et al. 2012). The Van der Waals interaction between carbon atom of CNT and oxygen atom of water molecule was described by the Lennard–Jones (L–J) potential $E = 4\varepsilon[(\sigma/r)^{12} - (\sigma/r)^6]$. Different L–J parameters were used to simulate the diverse contact angles of water on a flat graphene sheet (Werder et al. 2003). Here, we also used contact angle to indicate the strength of the interaction between the water and CNTs. All the Lennard–Jones potentials were cut off at 1 nm, and a long-range Coulombian interaction was calculated by a particle–particle–particle mesh (PPPM) solver (Hardy et al. 2009) with a relative error 0.0001 in forces. We controlled

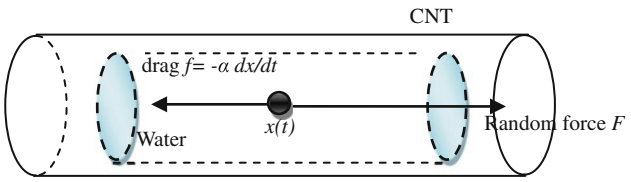

Fig. 1 Schematic diagram of water column's random motion in carbon nanotube

the tube temperature by applying Nose–Hoover thermal coupling (Nose 1984; Hoover 1985) with a relaxation time of 0.1 ps. The water temperature was not directly controlled; instead, it was maintained at a specific temperature through the heat exchange between the water and the CNTs. In order to keep the center of mass of the CNT at the original so that there is a reference point to easily determine the displacement of the water column, the displacement of the center of mass of the CNT was calculated and all atoms were shifted by this amount of displacement every time step. We assume that the displacement of the water column $x(t)$ is positive when the water column moves to the right of the CNT center. The time step size was 0.001 ps.

Figure 1 shows the schematic diagram of our simulation system. We adjusted the length of carbon nanotube L, the diameter of carbon tube d, the length of water column l, the contact angle θ_{CA} and the temperature T in our simulations. We used the tube length $L = 19.7$ nm so that it is at least 10 nm longer than the maximum length of the water column ($l = 10$ nm), providing enough separation distance between the two neighboring periodic images of the water column. We also investigated other CNTs with length of $L = 30$ and 40 nm and found that the effect of the nanotube length on the results was limited. Hence, in the rest of the simulations, the tube length $L = 19.7$ nm was adopted. Without loss of generality, we chose the parameter set $d = 2$ nm, $\theta_{CA} = 90°$ and $T = 298$ K as the standard reference case while varying column length l from 2 to 10 nm. In this standard parameter set, the armchair CNT (15, 15) was used.

Our MD simulations were carried out under NVT ensemble. After 100 ps, we started to record the random motion of water columns along the axial direction of the CNTs. It should be noted that during the simulations, no additional external force was applied to the water columns.

3 Simulation results and discussions

3.1 One-dimensional Brownian motion phenomenon

Figure 2a shows the effect of the water column length on the trajectory of the centre of mass of the water with the standard parameter set. The result indicates that the water column is constantly under random motion inside the CNT, even though no external force is applied onto the water. Figure 2b demonstrates the squared displacement of water columns as a function of time with each curve. As can be seen from Fig. 2b, the mean squared displacements (MSD) of the water columns generally increase with time linearly and the curves follow the diffusion theoretical prediction (Pathria 1996), namely, $\langle \Delta x^2 \rangle = 2Dt$, where D is diffusivity, regardless of water column length.

The velocity of each water column is a random variable. As in Fig. 3a, the velocity distributions of 2-, 3-, 4-, 6- and 10-nm-long water columns are compared with the normal distribution (dashed lines). The statistical average of the random velocity is almost zero regardless of the water column length, and the velocity fluctuation becomes weaker when the length of water column increases. Figure 3b demonstrates the quantitative analysis on the

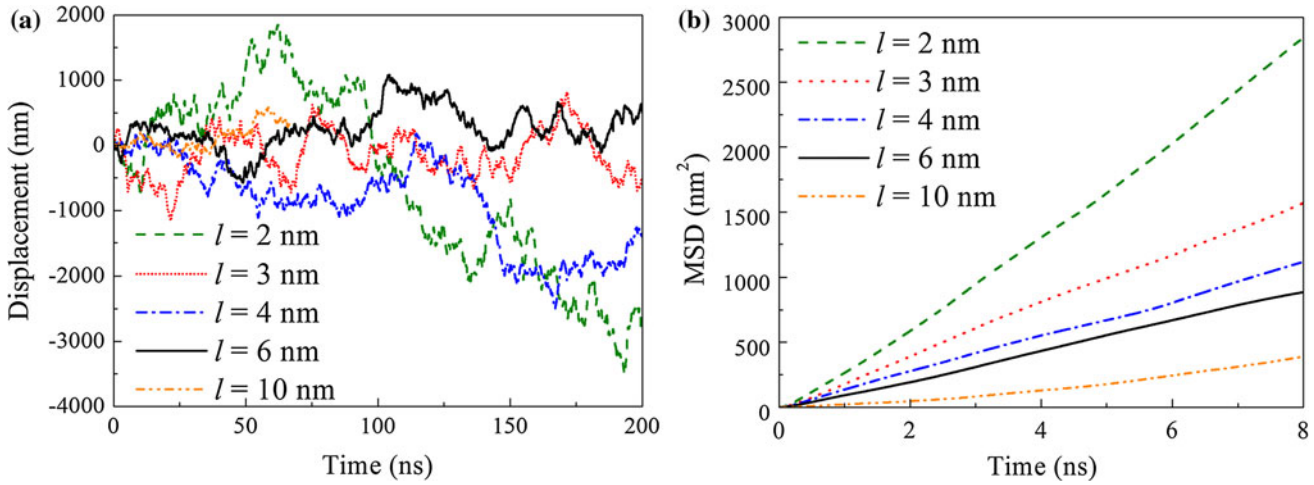

Fig. 2 **a** Displacement trajectories and **b** mean squared displacements of water columns with different length

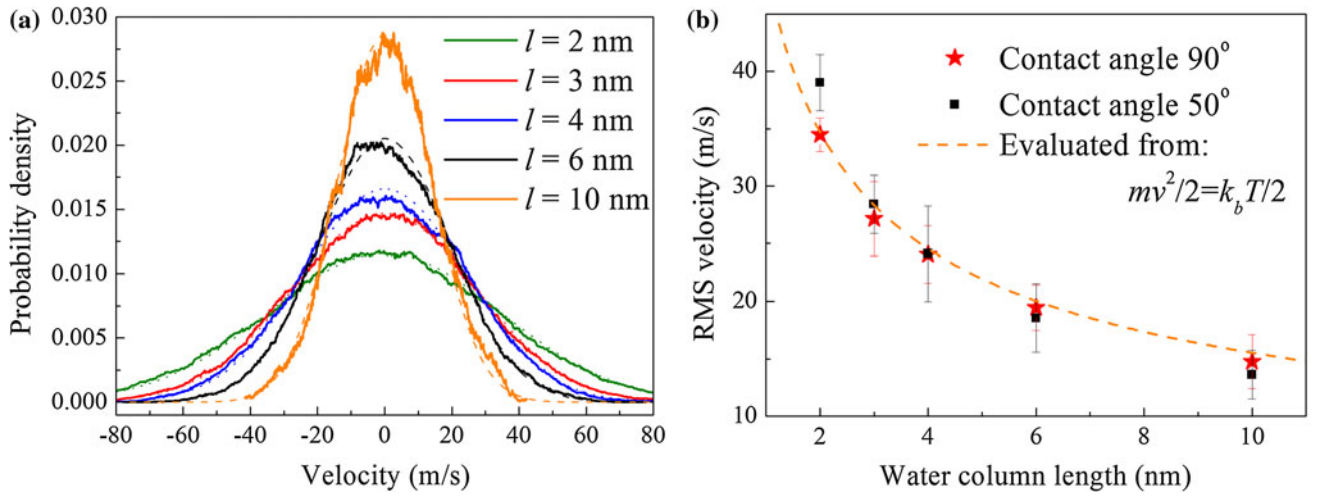

Fig. 3 **a** Probability density of the velocity of water columns, with the *dashed lines* representing the normal distributions; **b** RMS velocities of water columns with different length, and the *dashed line* is an estimation from the equipartition theorem

root-mean-square (RMS) velocity as a function of water column length. It appears that the velocity decreases with the increase in the water column length. The result is consistent with our intuition, namely the tendency of the random movement will continuously decrease as the length of water column increases. Hence, it is possible that the random movement of the center of mass of the water cannot be observed from a statistical point of view when a critical water column length is exceeded, although the local thermal fluctuations can still exist.

3.2 Random driving force of water inside CNTs

We then look into the driving force of the motion generated by the thermal activation. During the simulation, the temperature of the CNTs was maintained at 298 K and the carbon atoms kept on oscillating, which exerted a random force on the water molecules through carbon–water interactions. The probability distribution of the axial component of the random driving force is given in Fig. 4a. It can be found from Fig. 4a that the distribution of the force follows the normal distribution with a zero mean value, and the standard deviation (STD), which characterizes the magnitude of the random force varies with the simulated systems. The dependence of the STD on the length of water column is plotted in Fig. 4b. The root-square curve fitting of the standard deviation of the random force is $f_{\mathrm{STD}} = kl^{1/2}$, where the unit of force is nN, the length of water column is in nm, and k is a constant coefficient depending on the columns size,

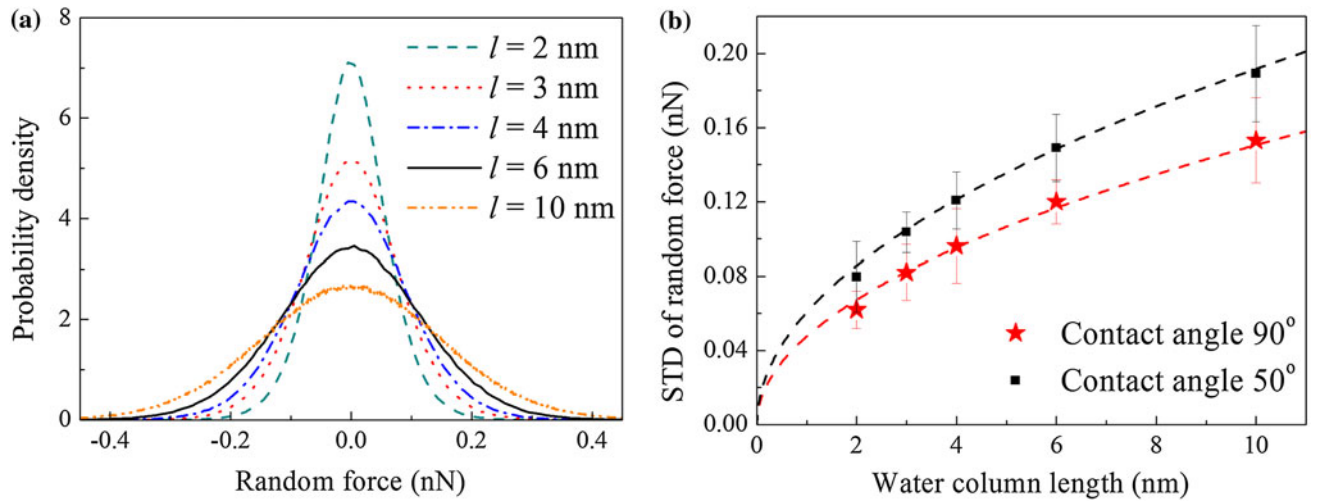

Fig. 4 **a** Probability density of the random force exerted on water column; **b** STD of random forces for water columns with different length, and the *dashed lines* are the fitting curves: $f_{\mathrm{STD}} = kl^{1/2}$

temperature and contact angle. The value of k is 0.048 nN nm$^{1/2}$ for the standard parameter set.

The reason we used the root-square law to fit STD of random forces is based on the following considerations: The random force is an extensive quantity whose fluctuation should be proportional to the square root of system size (Kadanoff 2000). So when the length of water column goes to zero, the random force should be zero too as expected. However, in current observation, when the water column is short (in the order of column diameter), the number of water molecules is small from the statistical point of view, which will cause the simulated results to deviate from its statistical predictions. This effect is minor for longer column length cases, and the relation holds better for larger system. Hence, $f_{\mathrm{STD}} = kl^{1/2}$ is a good approximation for the relationship between the random force and water length.

3.3 Instant mobility of water column

To investigate the characteristics of the one-dimensional Brownian motion of water columns inside the CNTs quantitatively, we then focus on the distance that the water columns can continuously slide along one direction. During the one-dimensional Brownian motion, the water columns can overcome the energy barrier and slip for a distance longer than the energy barrier periodic length L_{T}. The length of the energy fluctuation period L_T can be measured from Fig. 6a as 0.246 nm, which is consistent with the period of an armchair CNT atomic structure: $\sqrt{3}\sigma_{\mathrm{C-C}} = \sqrt{3} \times 0.142\ \mathrm{nm} = 0.246\ \mathrm{nm}$.

Because of the thermal fluctuation, the water columns can stop its continuous movement in one direction and move in the opposite direction. We define the distance for which the water column can move without changing its

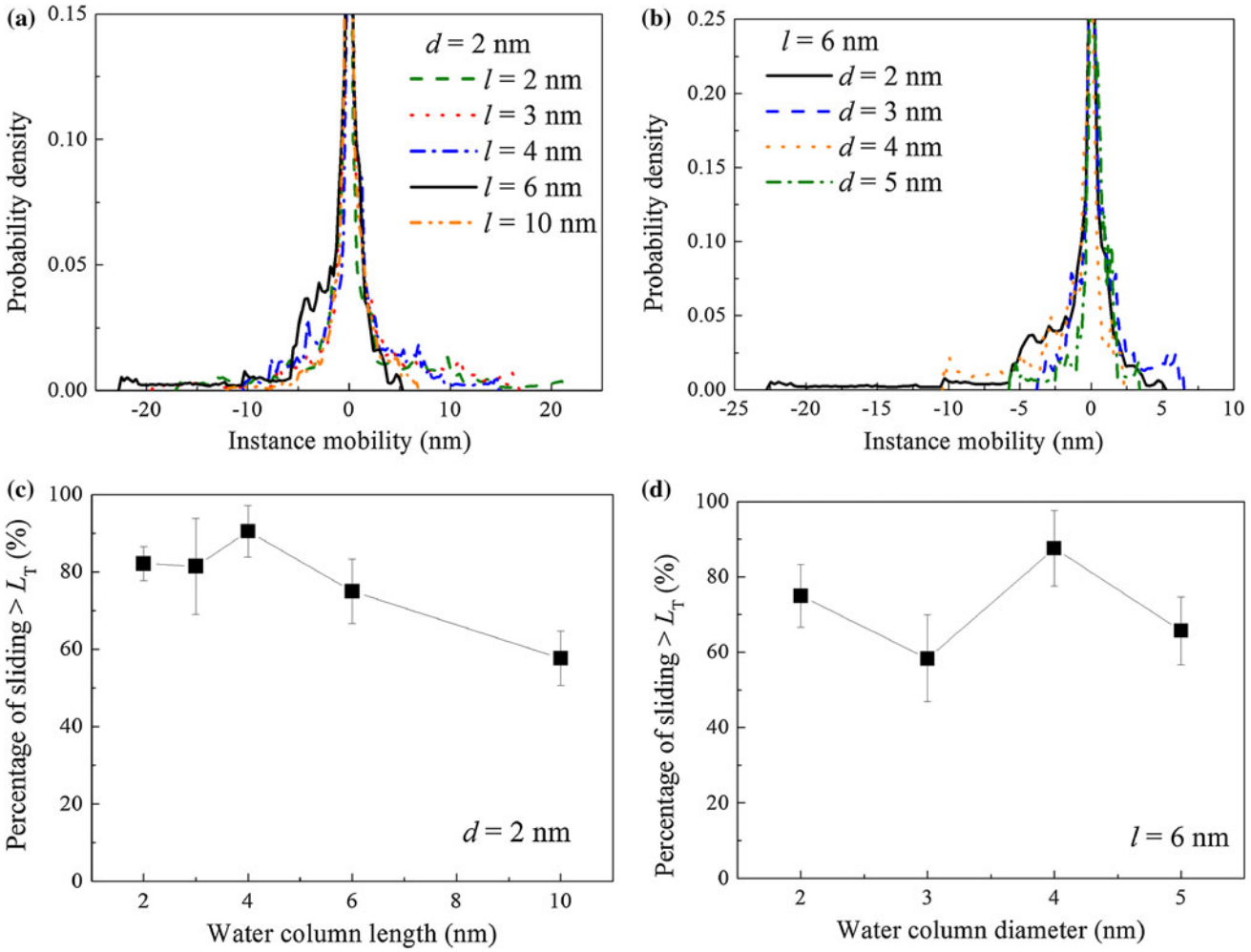

Fig. 5 Effects of **a** the water column length (with $d = 2$ nm) and **b** the CNT diameter (with $l = 6$ nm) on the distribution of the instant mobility (the parts of the curves with probability density larger than 0.15 are not shown). Dependence of the probability of the instant mobility exceeding the energy barrier period L_{T} on **c** the water column length (with $d = 2$ nm) and **d** the CNT diameter (with $l = 6$ nm)

direction as the instant mobility of the water column. Figure 5a, b demonstrates the effects of the water column length (with $d = 2$ nm) and CNT diameter (with $l = 6$ nm) on the distribution of the instant mobility, respectively. The probabilities of their instant mobility exceeding the energy barrier period L_T are provided in Fig. 5c, d, respectively. As can be seen from the figures, such a probability is always greater than 50 % with the given parameters, suggesting that these water columns could easily overcome the energy barrier and slide freely within the CNT at room temperature.

3.4 Energy barrier

As water moving inside the CNTs, it must overcome the energy barrier raised from the interactions between water molecules and carbon atoms. However, at room temperature, the thermal motion of individual water molecules is random and strong, so the direct measurement of the interaction between the water column and CNT is a very challenging task because the thermal noise level is orders higher than the energy barrier at room temperature. An extremely large number of independent simulations are required to increase the signal-to-noise ratio (Ma et al. 2011).

For the purpose of simplicity, we proposed a frozen water approach to reduce the thermal noise in water. The temperature of the water column was artificially reduced to extremely low, e.g., 1 and 0 K, so that the water columns were actually an ice block with little thermal fluctuation. As a result, when the water columns moved, the water molecules did not have sufficient mobility to quickly reach the minimal potential energy configuration. From this point of view, the energy barriers obtained using the proposed simulation will be upper bounds of the real values.

Figure 6a shows the potential energy between the water columns and CNTs as columns sliding at different position in the CNTs. The energy barrier obtained with the temperature of water column fixed at 0 K is around 50 % higher than those obtained with the temperature fixed at 1 K. It is reasonable to expect that the obtained energy barrier values are over-estimated in comparison with that at room temperature. Figure 6b shows that the energy barrier increases linearly with the water column length. For those

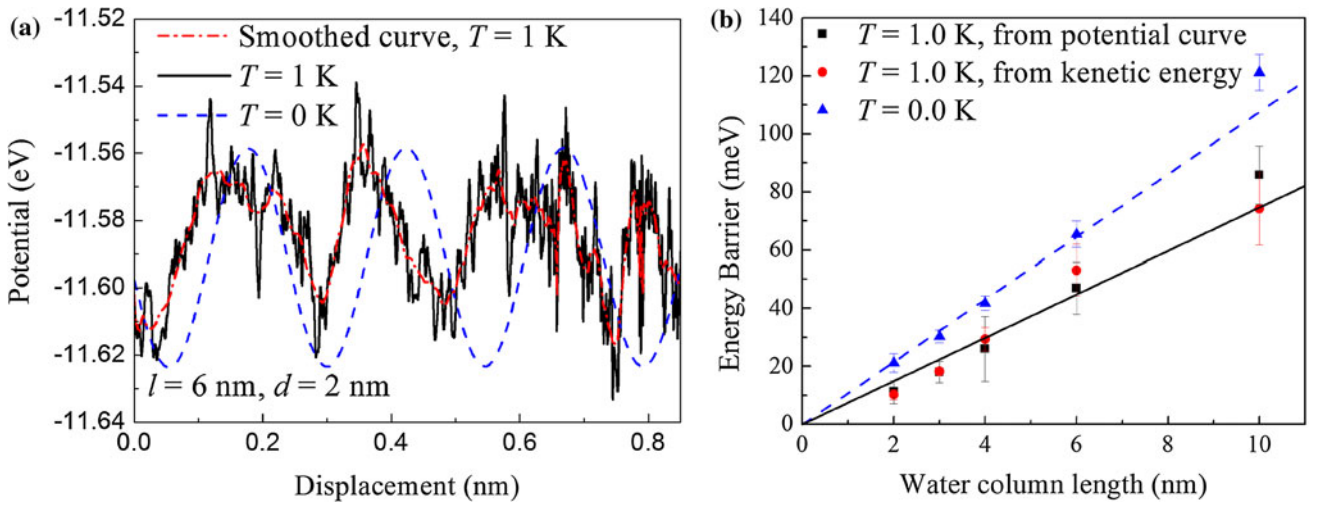

Fig. 6 **a** Fluctuation of the potential energy between the water and CNTs as the water column moves at low temperature; **b** the relationship between the energy barrier and the length of the water columns. The data points for temperature of 1 K are obtained based on the smoothed potential versus displacement curve in (**a**)

Table 1 Comparison between the driving and resistance forces

Length of water column l (nm)	Energy barrier $\Delta\varphi$ (meV)	Period of energy barrier L_T (nm)	Maximum drag force f_d (nN)	3 times standard deviation of driving force $3f_{STD}$ (nN)	$f_d/3f_{STD}$ (%)
2	10.22	0.246	0.02091	0.18603	11.24
3	18.05	0.246	0.03693	0.24615	15.00
4	26.02	0.246	0.05323	0.28863	18.44
6	46.88	0.246	0.09591	0.35979	26.66
10	74.13	0.246	0.15166	0.45913	33.03

obtained with water temperature fixed at 1 K, we have $\Delta\varphi = 6.5\ l$, where $\Delta\varphi$ is the energy barrier (in meV).

3.5 The critical length of a water column for a spontaneous slip driven by thermal fluctuation

We idealize the potential curve with a sinusoid: $\varphi(x) = \varphi_0 + (\Delta\varphi/2) \cdot \sin(2\pi x/L_T)$, where x is position of column, then the first derivative gives the estimation of the maximum drag force exerted on the frozen water column: $f_d = \pi\Delta\varphi/L_T$.

Thermal driving force is a random variable and follows the normal distribution. The probabilities of the magnitude of driving force exceeding its STD (f_{STD}), $2f_{STD}$ and $3f_{STD}$ are 31.74, 4.56 and 0.26 %, respectively. Due to the extremely large number of attempts (in the order of a couple of attempts per picosecond), the total times of the driving force exceeding $3f_{STD}$ are still very high from the macroscopic point of view.

Table 1 reports the comparison between the random driving force due to thermal fluctuation- and the energy barrier-induced resistance force. We find from the table that the maximum drag force is only about 10–30 % of $3f_{STD}$. The above comparison is a conservative evaluation because of the following two reasons. First, the energy barrier from the frozen water column model in the simulation leads to a significantly overestimated resistance force. Second, the probability of the random forces exceeding $3f_{STD}$ is 0.26 %, which is still very likely to occur due to the extremely large number of attempts in a longtime observation period. The significance is, even based on this conservative estimation, the random driving force is able to overcome the upper bound of the flow resistance in the simulated systems. Therefore, the slip of the water column in the CNT without external force is inevitable.

We further approximately estimate the critical length, below which the vibration of the water column will spontaneously occur at room temperature. Using the simulation results based on the standard parameter set, we extrapolate the random driving force using the root-square law and the resistance using the linear law as shown in Fig. 7. The intersection of the two curves indicates the maximum length of the water column, under which the water column will experience the apparent one-dimensional Brownian motion at room temperature. According to Fig. 7, for a water column inside a CNT with diameter of 2 nm at temperature 300 K, the critical length estimated here is around 117 nm. Because of the overestimation of the drag force and the underestimation of the driving force, the calculated critical length here is the lower bound of the true value.

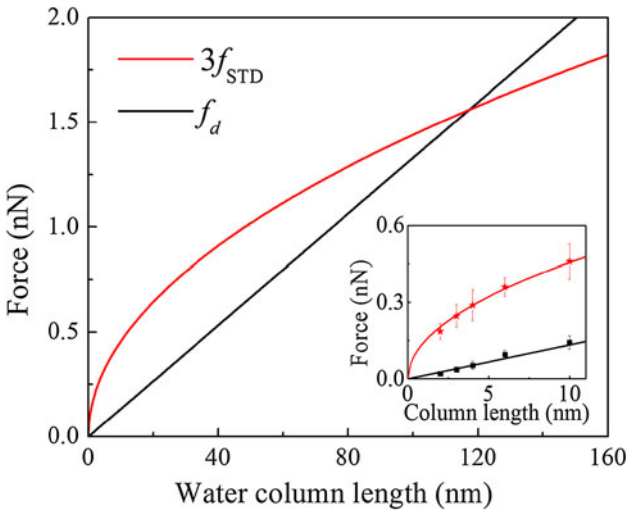

Fig. 7 Prediction of the maximum length under which the Brownian motion of water column occurs

3.6 Parametric study

In order to study the effect of the CNT size on the one-dimensional motion of water column, we changed the diameter of the CNTs from 2 to 5 nm in the MD simulations. The effect of the tube diameter on the random motion velocity and random force is demonstrated in Fig. 8a. It can be seen from the figure that the mean square velocity of water column decreases and the standard deviation of the random force increases as the tube diameter increases. Temperature is the key element to induce the Brownian motion. Figure 8b presents the effect of temperature on the mean square velocity and the standard deviation of the corresponding random force. It is observed from Fig. 8b that both the mean square velocity and the standard deviation of random force slightly increase as the temperature increases, which is consistent with the expectation. However, the increase is not significant when temperature changes from 275 to 298 K.

In our MD simulations, the Van der Waals interaction between the CNT and water molecules is represented by the Lennard–Jones (L–J) potential model between the carbon and oxygen atoms. Since the contact angle θ_{CA} is directly related to the adhesion strength between the CNT and water (Xiong et al. 2013), we here quantify the interaction strength through θ_{CA}, namely the L–J potential is calibrated to produce specific contact angles. In the one-dimensional Brownian motion simulations, we changed the contact angle from hydrophilic to hydrophobic by adjusting the parameters in the L–J potential model. The effect of the contact angle on the random motion velocity and random force of water column with $l = 6$ nm and $d = 2$ nm is shown in Fig. 8c. The random force decreases when the

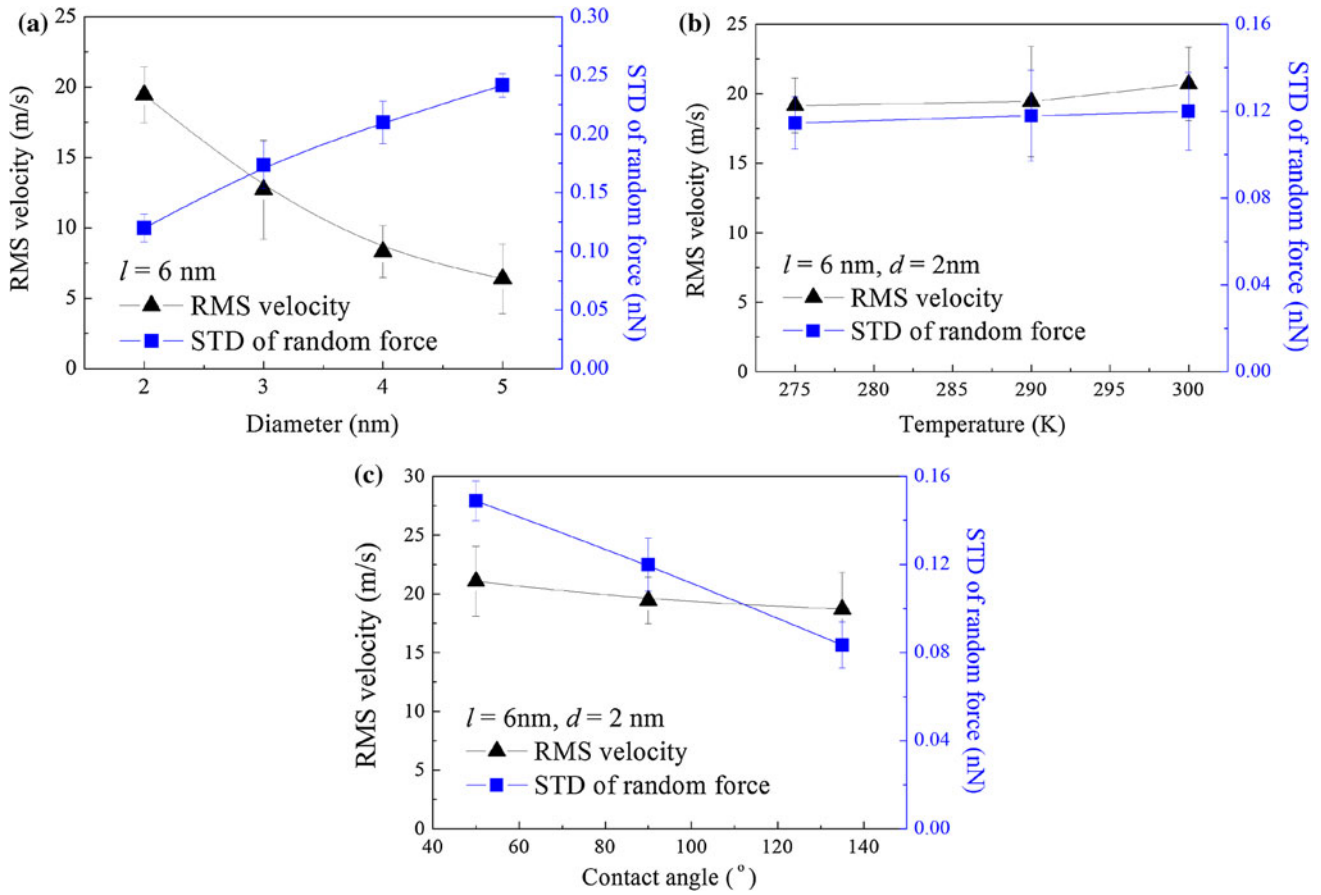

Fig. 8 Effects of **a** CNT diameter, **b** temperature, and **c** contact angle on the random motion velocity and random force of water column

interaction weakens (toward hydrophobic), and there is approximately a linear relationship between the random force and the contact angle. The RMS velocity is slightly affected by the contact angle since the main contribution to the RMS velocity is thermal energy $kT/2$.

4 Conclusions

In this study, the slip behavior of water at atomically smooth carbon nanotube wall is investigated from a special point of view. By simulating the short-term one-dimensional Brownian motions of water columns inside CNTs, we obtain the thorough characteristics of the water column vibration. It is confirmed that although water molecules form layered structures near the CNT walls, nanoscale water columns do have the ability to slip at atomically smooth surface spontaneously caused by the thermal activation at room temperature. By comparing the thermal fluctuation-induced random driving force and potential energy-induced resistance, we predict the lower bound of the critical water column length conservatively, under which the slip of water column inside carbon nanotube can spontaneously occur under any given pressure drop at room temperature.

Acknowledgments L.S. acknowledges the financial support from the University of Sydney through the International Program Development Fund. Q.Z. appreciates the support by the National Science Foundation of China (NSFC) through Grant No. 10672089, No. 10772100 and No. 10832005, and the 973 Program No. 2007CB936803. The authors are grateful to the computing support from NCI National Facilities in Australia.

References

Barthlott W, Neinhuis C (1997) Purity of the sacred lotus, or escape from contamination in biological surfaces. Planta 202:1–8

Berendsen HJC, Grigera JR, Straatsma TP (1987) The missing term in effective pair potentials. J Phys Chem 91:6269–6271

Chen X, Cao GX, Han AJ, Punyamurtula VK, Liu L, Culligan PJ, Kim T, Qiao Y (2008) Nanoscale fluid transport: size and rate effects. Nano Lett 8:2988–2992

Chen C, Ma M, Jin K, Liu JZ, Shen L, Zheng Q, Xu Z (2011) Nanoscale fluid-structure interaction: flow resistance and energy transfer between water and carbon nanotubes. Phys Rev E 84:046314

Gonzalez MA, Abascal JLF (2010) The shear viscosity of rigid water models. J Chem Phys 132:096101

Hardy DJ, Stone JE, Schulten K (2009) Multilevel summation of electrostatic potentials using graphics processing units. Parallel Comput 35(3):164–177

Holt JK, Park HG, Wang YM, Stadermann M, Artyukhin AB, Grigoropoulos CP, Noy A, Bakajin O (2006) Fast mass transport through sub-2-nanometer carbon nanotubes. Science 312:1034–1037

Hoover WG (1985) Canonical dynamics: equilibrium phase-space distributions. Phys Rev A 31(3):1695–1697

Kadanoff LP (2000) Statistical physics: statics, dynamics and renormalization. World Scientific. http://www.worldscientific.com/worldscibooks/10.1142/4016

Ma MD, Shen L, Sheridan J, Liu JZ, Chen C, Zheng Q (2011) Friction of water slipping in carbon nanotubes. Phys Rev E 83(3):036316

Majumder M, Chopra N, Andrews R, Hinds BJ (2005) Nanoscale hydrodynamics—enhanced flow in carbon nanotubes. Nat 438(7064):44

Markesteijn AP, Hartkamp R, Luding S and Westerweel J (2012) A comparison of the value of viscosity for several water models using Poiseuille flow in a nano-channel. J Chem Phys 136:134104

Martini A, Hsu HY, Patankar NA, Lichter S (2008) Slip at high shear rates. Phys Rev Lett 100:206001

Mo H, Evmenenko G, Dutta P (2005) Ordering of liquid squalane near a solid surface. Chem Phys Lett 415:106–109

Nose S (1984) A molecular dynamics method for simulations in the canonical ensemble. Mol Phys 52:255–268

Pathria RK (1996) Statistical mechanics. Butterworth-Heinemann, UK

Peng XS, Jin J, Nakamura Y, Ohno T, Ichinose I (2009) Ultrafast permeation of water through protein-based membranes. Nat Nanotechnol 4:353–357

Plimpton S (1995) Fast parallel algorithms for short-range molecular-dynamics. J Comput Phys 117:1–19

Stone HA, Stroock AD, Ajdari A (2004) Engineering flows in small devices: microfluidics toward a lab-on-a-chip. Annu Rev Fluid Mech 36:381–411

Stuart SJ, Tutein AB, Harrison JA (2000) A reactive potential for hydrocarbons with intermolecular interactions. J Chem Phys 112:6472

Thompson PA, Troian SM (1997) A general boundary condition for liquid flow at solid surfaces. Nature 389:360–362

Werder T, Walther JH, Jaffe RL, Halicioglu T, Koumoutsakos P (2003) On the water-carbon interaction for use in MD simulations of graphite and carbon nanotubes. J Phys Chem B 107:1345–1352

Xiong W, Liu JZ, Ma M, Xu ZP, Sheridan J, Zheng QS (2011) Strain engineering water transport in graphene nanochannels. Phys Rev E 84:056329

Xiong W, Liu JZ, Zhang ZL, and Zheng QS (2013) Control of surface wettability via strain engineering. arXiv:1304.4770

Yang F (2009) Slip boundary condition for viscous flow over solid surface—a rate process. Chem Eng Commun 197:544–550